

(1) Ab initio Hartree-Fock calculations at the double- ζ level show all hexahalogenated benzenes to be planar. It is highly unlikely that this result is an artifact of the approximations used.

(2) Deviations from planarity observed in the solid state are well within the range of crystal packing forces and are not caused by steric overcrowding.

(3) Spectroscopic investigations indicate that the deviation from planarity in vapor should be no larger than in the solid state.

(4) Electron diffraction investigations claim C_6Br_6 to be significantly nonplanar in the gas phase, contrary to our conclusions above. We suggest a redetermination of this structure with

present-day tools. A GED investigation on C_6I_6 , hitherto not attempted, is also within reach and would provide data of vital interest for the subject studied here.

Acknowledgment. We thank Dr. Tor Strand for many valuable discussions regarding the conformations of hexahalobenzenes. We are also indebted to Dr. R. Johansen and Dr. K. Løchsen at Norsk Data A/S and to Dr. B. Schilling at this institute for assistance with some of the calculations.

Registry No. C_6H_6 , 71-43-2; C_6F_6 , 392-56-3; C_6Cl_6 , 118-74-1; C_6Br_6 , 87-82-1; C_6I_6 , 608-74-2.

Photoelectron Spectroscopy of the Allenyl Ion $CH_2=C=CH^-$

John M. Oakes and G. Barney Ellison*

Contribution from the Department of Chemistry, University of Colorado,
Boulder, Colorado 80309. Received December 21, 1982

Abstract: We have studied the photodetachment spectra of $CH_2=C=CH^-$, $CD_2=C=CH^-$, and $CH_2=C=CD^-$. By comparing the photoelectron spectra of these selectively labeled species, we conclude that the ion has an allenyl (rather than propargyl) structure. The electron affinities (EA) of a set of propargyl radicals are as follows: $EA(CH_2C\equiv CH) = 0.893 \pm 0.025$ eV, $EA(CD_2C\equiv CH) = 0.907 \pm 0.023$ eV, and $EA(CH_2C\equiv CD) = 0.88 \pm 0.15$ eV. A single active vibration is observed in the photoelectron spectra of $CH_2=C=CH^-$ and $CD_2=C=CH^-$. This mode has a frequency of 510 cm^{-1} and is assigned as an out-of-plane bend of the acetylenic hydrogen of the propargyl radical (either $CH_2C\equiv CH$ or $CD_2C\equiv CH$). The gas-phase acidity of allene and methylacetylene are reported as $\Delta H^\circ_{\text{acid}}(H-CH_2CCH) = 382.3 \pm 1.2$ kcal/mol and $\Delta H^\circ_{\text{acid}}(H-CH=C=CH_2) = 380.7 \pm 1.2$ kcal/mol. The $\Delta H^\circ_{298}(CH_2=C=CH^-)$ is 59.4 ± 1.2 kcal/mol.

Introduction

The propargyl radical ($CH_2C\equiv CH$) is of great interest to many chemists because it is one of the simplest conjugated organic radicals. For this reason, there has been much effort to determine its "resonance energy" and heat of formation.¹⁻⁴ The radical C_3H_3 was first observed, and its ionization potential measured, by Farmer and Lossing⁵ in 1955 from the thermal decomposition of propargyl iodide ($HC\equiv CCH_2I$). In addition, the electronic absorption spectrum of C_3H_3 has been observed⁶ in gas-phase flash photolysis, as well as in matrix isolation⁷ experiments. From the electronic spectra, several vibrational modes were extracted, although not definitely assigned.

Relatively little is known about the corresponding anion, $C_3H_3^-$. The gas-phase acidity of methylacetylene ($CH_3C\equiv CH$) has been measured^{8,9} as 379.6 ± 2 kcal/mol. However, due to the coincidentally close acidities of the methyl hydrogens and the acetylenic hydrogen,¹⁰ it was difficult to be sure which of the $C_3H_3^-$ isomers

was produced in the experiment. In fact, attack by a base on $CD_3C\equiv CH$ has been shown^{11,12} in the gas phase to produce both CD_2CCH^- and $CD_3C\equiv C^-$. Fluoride ion displacement on $(C-H_3)_3SiC\equiv CCH_3$ and $HC\equiv CCH_2Si(CH_3)_3$ in a flowing after-glow¹³ has separately produced the $CH_3C\equiv C^-$ and CH_2CCH^- ions. The chemistry of these isomeric ions has been shown to differ.¹⁴

We have used the method of negative ion photoelectron spectroscopy¹⁵ to study the photodetachment of a mass-selected (m/z 39) negative ion beam produced by using methylacetylene or allene as ion precursors. In this experiment, a fixed-frequency argon ion laser is crossed with the ion beam, and the kinetic energy of the resulting detached electrons is measured. In order to determine which of the two possible isomers of the m/z 39 ion (i.e., $CH_3C\equiv C^-$ or CH_2CCH^-) is being observed in detachment, we have also used $CH_3C\equiv CD$ and $CD_3C\equiv CH$ as ion precursors. If hydrogen/deuterium (H/D) scrambling does not occur, we can separate the two isomers [e.g., $CH_3C\equiv CD \rightarrow CH_3C\equiv C^-$ (m/z 39) and CH_2CCD^- (m/z 40)] to decide which species is detaching. We conclude that the observed photodetachment spectrum results exclusively from CH_2CCH^- . In addition, by observing the effect

- (1) W. Tsang, *Int. J. Chem. Kinet.*, **2**, 23 (1970).
- (2) K. D. King, *Int. J. Chem. Kinet.*, **10**, 545 (1978).
- (3) K. D. King and T. T. Nguyen, *J. Phys. Chem.*, **83**, 1940 (1979).
- (4) K. Sen Sharma and J. L. Franklin, *J. Am. Chem. Soc.*, **95**, 6562 (1973).
- (5) J. B. Farmer and F. P. Lossing, *Can. J. Chem.*, **33**, 861 (1955).
- (6) D. A. Ramsay and P. Thistlethwaite, *Can. J. Phys.*, **44**, 1381 (1966).
- (7) M. E. Jacox and D. E. Milligan, *Chem. Phys.*, **4**, 45 (1974).
- (8) J. E. Bartmess, J. A. Scott, and R. T. McIver, Jr., *J. Am. Chem. Soc.*, **101**, 6046 (1979).
- (9) J. E. Bartmess and R. T. McIver, Jr., in "Gas Phase Ion Chemistry", Vol. II, M. T. Bowers, Ed., Academic Press, New York, 1979, p 153-179.
- (10) J. E. Bartmess, private communication, 1982.

- (11) J. H. Stewart, R. H. Shapiro, C. H. Depuy, and V. M. Bierbaum, *J. Am. Chem. Soc.*, **99**, 7650 (1977).
- (12) J. H. J. Dawson, T. A. M. Kaandorp, and N. M. M. Nibbering, *Org. Mass. Spectrom.*, **12**, 330 (1977).
- (13) C. H. DePuy, V. M. Bierbaum, L. A. Flippin, J. J. Grabowski, and G. K. King, *J. Am. Chem. Soc.*, **102**, 5012 (1980).
- (14) G. K. King, M. M. Maricq, V. M. Bierbaum, and C. H. DePuy, *J. Am. Chem. Soc.*, **103**, 7133 (1981).
- (15) M. W. Siegel, R. J. Celotta, J. L. Hall, J. Levine, and R. A. Bennett, *Phys. Rev. A*, **6**, 607 (1972).

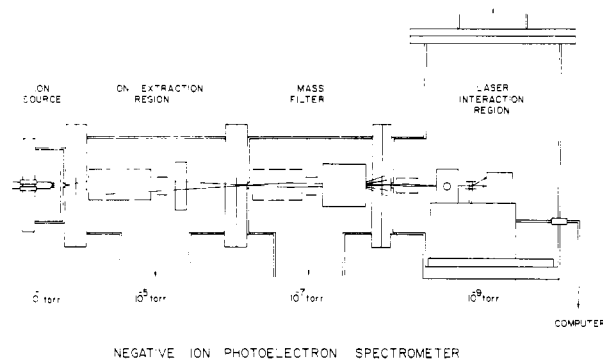


Figure 1. Schematic diagram of the negative ion photoelectron spectrometer used for this experiment.

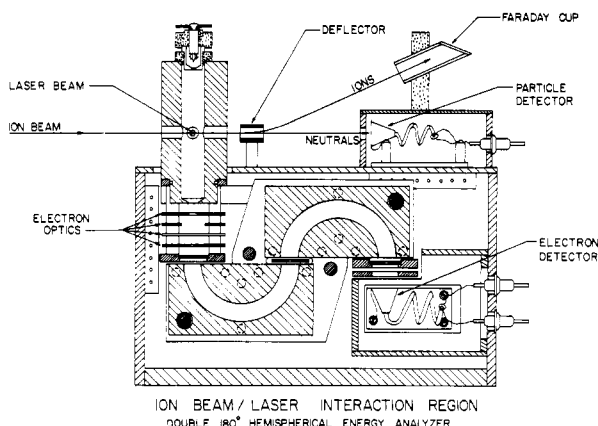


Figure 2. Cross-sectional diagram of the electron-energy analyzer and the laser/ion beam interaction region.

of selective deuteration on the photodetachment spectrum of this ion, we have gained insight into its structure. We find it to be allenyl ($\text{CH}_2=\text{C}=\text{CH}^-$), rather than propargyl ($^-\text{CH}_2\text{C}\equiv\text{CH}$). Finally, we are able to determine the electron affinities of the molecules CH_2CCH , CH_2CCD , and CD_2CCH , as well as other resulting thermodynamic information.

Experimental Section

The apparatus used to collect the photodetachment data has been carefully described previously.¹⁶ Figure 1 shows a schematic diagram of the machine. Briefly, a mixture of parent gases is allowed to flow into a high-pressure (roughly 0.1 torr), magnetically confined discharge ion source. This source is floated at the desired beam energy (600 V in this experiment). The negative ions that are extracted through a 1-mm aperture are formed into a beam in the first high-vacuum region (10^{-5} torr). A set of perpendicular deflectors directs the beam through a 2-mm aperture into the second high-vacuum region (10^{-7} torr). The beam is refocused and passed through a Wien filter, which disperses the ion beam according to velocity. Because all of the ions are born at -600 V, this velocity selection results in mass selection. The dispersed beam is incident upon a $0.5\text{ mm} \times 2\text{ mm}$ slit, giving a mass resolution of approximately $m/\Delta m = 50$. This mass selected beam then centers the final high-vacuum region (10^{-9} torr) where a final einzel lens focuses it into the laser/ion beam interaction region.

The mass selected ion beam is intersected at a 90° angle by a fixed, single-frequency laser beam from an argon ion laser (Spectra Physics Model 170). The laser is used in an intracavity mode, giving approximately 75 W of continuous power at $\lambda_0 = 488\text{ nm}$. Those electrons resulting from laser-induced detachment which are scattered at 90° to both the laser and ion beams enter the electron-energy analyzer (see Figure 2). The aperture accepts approximately $4\pi/1500$ of the total number of electrons detached. The electrons entering the analyzer are focused and deflected onto a 0.5-mm slit. The electrons then enter the double-hemispherical energy analyzer. The kinetic energy (KE) of the electron at this point is given by $\text{KE} = \text{KE}_{\text{init}} + V_{\text{slit}}$, where KE_{init} is the kinetic energy of the detached electron ($0 \leq \text{KE}_{\text{init}} \leq \hbar\omega_0$, where $\hbar\omega_0$ is the laser energy, usually 2.540 eV), and V_{slit} is the voltage on the slit

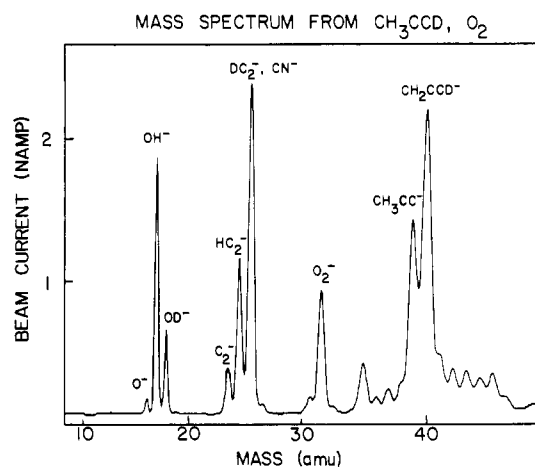


Figure 3. Typical mass spectrum obtained from the Wien filter. The mass resolution is approximately $m/\Delta m = 50$.

at the entrance to the hemispheres. The voltage across the hemispheres is constant, giving a set transmission energy (roughly 4.0 eV). Those electrons passing through both hemispheres and the final slit enter a Ceratron electron multiplier. In order to scan the electron spectrum, a computer is used to successively ramp V_{slit} and count the number of pulses from the electron multiplier. Many successive scans are performed until a sufficient signal-to-noise ratio is obtained (1–3 h). The energy resolution (fwhm) of our electron-energy analyzer is $20\text{--}25\text{ meV}$.

A small correction (of the order of 10 meV) must be made to our raw data due to a center of mass transformation. Our measurements are performed in the laboratory frame, but detachment occurs in the center of mass (COM) frame. In order to extract the COM kinetic energy from the slit voltages read by the computer, we use eq 1,¹⁵ where KE is the COM

$$\text{KE} = \text{KE}_{\text{cal}} + \gamma(V - V_{\text{cal}}) + mW(1/M_{\text{cal}} - 1/M) \quad (1)$$

kinetic energy (eV) of an electron detached from an ion of mass M (amu), V is the slit voltage at which the electron passes through the analyzer, and KE_{cal} is the COM kinetic energy of the calibration ion of mass M_{cal} . The slit voltage at the center of the peak in the PES of the calibration ion is V_{cal} , while γ is a unitless energy-scale compression factor measured from the PES¹⁷ of NH^- . Normally we measure γ to be 1.00 ± 0.03 . W is the ion beam energy (600 V), and m is the mass of the electron.

For the experiment in question, an approximately 1:1 mixture of the desired hydrocarbon and O_2 was used, along with a 0.015-in. tungsten filament. The allene ($\text{CH}_2=\text{C}=\text{CH}_2$) and methylacetylene ($\text{CH}_3\text{C}\equiv\text{CH}$) were supplied by Air Products, and the methylacetylene- d_3 ($\text{CD}_3\text{C}\equiv\text{CH}$) was supplied by Merck, Sharpe and Dohme. All were used as supplied. Indeed, one nice feature of this experiment is that highly pure ion precursors are not normally necessary because in the process of ion mass selection, any unwanted ions resulting from impurities are generally eliminated.

The methylacetylene- d_1 ($\text{CH}_3\text{C}\equiv\text{CD}$) was synthesized by adding methylacetylene to Et_2O at -78°C followed by a stoichiometric amount of CH_3Li . At ambient temperature, D_2O was added, and evolved methylacetylene- d_1 was collected at -78°C . This product was bulb-to-bulb distilled to remove Et_2O , and several freeze-pump-thaw cycles were performed to remove volatile impurities. The purity was confirmed¹⁸ by the disappearance of the acetylenic hydrogen infrared absorption at 3334 cm^{-1} and the appearance of the corresponding deuterium stretch at 2616 cm^{-1} .

Because identification of the $\text{C}_3\text{H}_n\text{D}_{3-n}^-$ ions is so important to this experiment, some discussion of our mass spectra is called for. From methylacetylene and O_2 , approximately 3 nA of an ion of $m/z\ 39$ is obtained. The mass resolution is good enough to rule out interference in the spectrum from large amounts of an ion of $m/z\ 40$ or 38 . The Wien filter is set to the top of the peak corresponding to $m/z\ 39$, and a photoelectron spectrum (PES) is taken. Calibration of the mass spectrum is achieved by looking on the same day at the PES of the ions of $m/z\ 43$ ($\text{C}_2\text{H}_3\text{O}^-$) and $m/z\ 45$ ($\text{C}_2\text{H}_5\text{O}^-$). Both of these may be identified according to their photoelectron spectra.¹⁹ In addition, a PES of OH^- (m/z

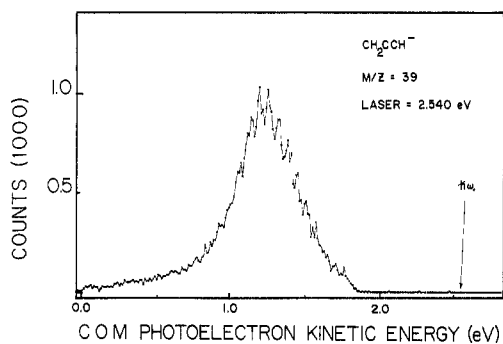
(17) P. C. Engelking and W. C. Lineberger, *J. Chem. Phys.*, **65**, 4323 (1976).

(18) T. Shimanouchi, "Table of Molecular Vibrational Frequencies", Vol. I, National Bureau of Standards, Washington, DC, 1972.

(16) H. B. Ellis, Jr., and G. B. Ellison, *J. Chem. Phys.*, in press.

Table I. Ion Identification Scheme

precursor	ion	m/z	detach- ment?
$\text{CH}_3\text{C}\equiv\text{CH}$	CH_2CCH^- CH_3CC^-	39	yes
$\text{CH}_2=\text{C}=\text{CH}_2$	CH_2CCH^- $\text{CH}_3\text{CC}(?)$	39	yes
$\text{CH}_3\text{C}\equiv\text{CD}$	CH_2CCD^- CH_3CC^-	40 39	yes no
$\text{CD}_3\text{C}\equiv\text{CH}$	CD_2CCH^- CD_3CC^-	41 42	yes no

Figure 4. Low-resolution (11.0 meV per data point) photoelectron spectrum of the ion CH_2CCH^- obtained from $\text{CH}_3\text{C}\equiv\text{CH}/\text{O}_2$.

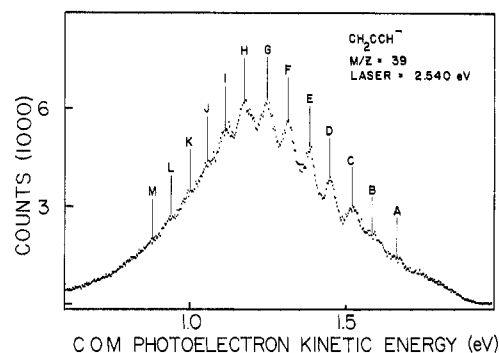
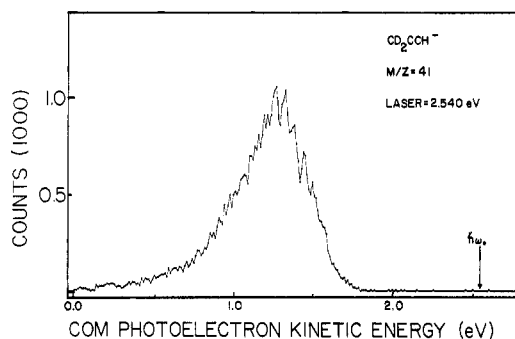
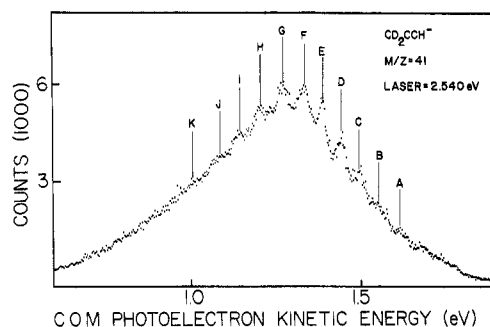
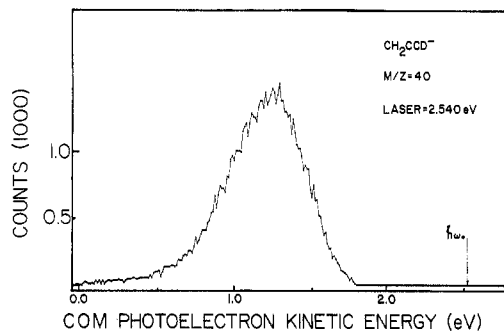
17) and O^- (m/z 16) is taken in order to calibrate the electron spectrometer for C_3H_3^- (see Results) and help identify the mass of the ion in question. There is also an O_2^- (m/z 32) peak, which can be used to calibrate our mass spectrum as well, because its photoelectron spectrum is well-known.²⁰

A typical mass spectrum from $\text{CH}_3\text{C}\equiv\text{CD}$ and O_2 is shown in Figure 3. The same ions are used to calibrate the masses in this spectrum as described for $\text{CH}_3\text{C}\equiv\text{CH}/\text{O}_2$ above. In addition, a peak is seen from OD^- (m/z 18), as expected. The mass peaks of interest in this spectrum are those at m/z 39, preliminarily assigned as $\text{CH}_3\text{C}\equiv\text{C}^-$, and at m/z 40, preliminarily assigned as CH_2CCD^- . If no H/D scrambling occurs within the source, these are the most probable structural formulas for these ions. In order to confirm this, V_{slit} is set manually to a peak where it is known that C_3H_3^- detachment affords a considerable count rate. The number of electron counts per second per nanoamperes of ions per watt of laser power ($\text{count}\cdot\text{s}^{-1}\cdot\text{nA}^{-1}\cdot\text{W}^{-1}$) for the two peaks (m/z 39 and 40) is recorded. We will demonstrate below that essentially only one of the C_3H_3^- isomers detaches. This provides us with a means to investigate the degree of H/D scrambling. Note in Figure 3 that the mass resolution is sufficient for separation of the m/z 39 and 40 components.

The mass spectrum obtained from $\text{CD}_3\text{C}\equiv\text{CH}$ and O_2 is very similar in overall appearance to that from $\text{CH}_3\text{C}\equiv\text{CD}$, with the exception that the two important ions are now m/z 40 and 41, preliminarily assigned as CD_2CCH^- and CD_3CC^- , respectively.

Results

As mentioned earlier, an absolute identity of the ions being detached in this experiment is essential. The results of attempts to estimate the degree of H/D exchange in our ion source follow. Beginning with the results from $\text{CH}_3\text{C}\equiv\text{CD}$, we measured the electron count rate at a set V_{slit} and laser power. The result was that a 2-nA beam of the ions of m/z 40 gave 100 counts/s, while a 1.3-nA beam of the ions of m/z 39 gave 12 counts/s. Note that the background counting rate, with the ion beam off and the laser on is roughly 1 count/s. Assuming that the ion CH_2CCH^- and its deuterated isomers have the same cross section for photodetachment, we conclude that the degree of H/D scrambling within the molecules is $\leq 15\%$, i.e., that the ion current corresponding to m/z 39 from $\text{CH}_3\text{C}\equiv\text{CD}$ is $\geq 85\%$ $\text{CH}_3\text{C}\equiv\text{C}^-$ and that the ion current corresponding to m/z 40 from the same precursor is $\geq 85\%$ CH_2CCD^- . This is probably a conservative estimate because most

Figure 5. High resolution (2.7 meV per data point) photoelectron spectrum of the ion CH_2CCH^- obtained from $\text{CH}_3\text{C}\equiv\text{CH}/\text{O}_2$.Figure 6. Low-resolution (11.0 meV per data point) photoelectron spectrum of the ion CD_2CCH^- obtained from $\text{CD}_3\text{C}\equiv\text{CH}/\text{O}_2$.Figure 7. High-resolution (2.7 meV per data point) photoelectron spectrum of the ion CD_2CCH^- obtained from $\text{CD}_3\text{C}\equiv\text{CH}/\text{O}_2$.Figure 8. Low-resolution (11.0 meV per data point) photoelectron spectrum of the ion CH_2CCD^- obtained from $\text{CH}_3\text{C}\equiv\text{CD}/\text{O}_2$.

of the 12 counts/s in the m/z 39 peak could be explained as contamination in the m/z 39 beam from ions of m/z 40 due to imperfect mass selection.

It is concluded that all of the detachment in our spectrum can be attributed to the CH_2CCH^- ion and that the methylacetylide ion ($\text{CH}_3\text{C}\equiv\text{C}^-$) does not detach with 488-nm photons. We have seen no evidence for detachment of the methylacetylide radical. This might be expected, because the methylacetylide radical is estimated to have a relatively high electron affinity (EA). The electron

(19) G. B. Ellison, P. C. Engelking, and W. C. Lineberger, *J. Phys. Chem.*, **86**, 4873 (1982).

(20) R. J. Celotta, R. A. Bennett, J. L. Hall, M. W. Siegel, and J. Levine, *Phys. Rev. A*, **6**, 631 (1972).

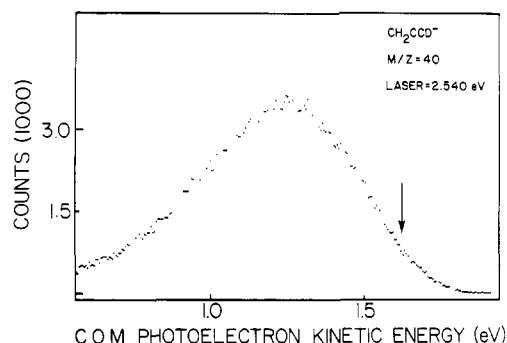


Figure 9. High-resolution (5.5 meV per data point) photoelectron spectrum of the ion CH_2CCD^- obtained from $\text{CH}_3\text{C}\equiv\text{CD}/\text{O}_2$.

affinity of this radical is probably not greatly different from that of $\text{HC}\equiv\text{C}$, the only difference being the substitution of a methyl group for hydrogen. The EA of $\text{HC}\equiv\text{C}$ has been measured²¹ and is 2.94 ± 0.10 eV.

To help confirm the high EA of $\text{CH}_3\text{C}\equiv\text{C}$, we examined the m/z 39 ion from $\text{CH}_3\text{C}\equiv\text{CD}/\text{O}_2$ with the highest energy laser line available to us (457.9 nm, or 2.707 eV). No detachment was detected. This laser line was approximately one-fifth of the power of the 488-nm (2.540 eV) line we normally use. Nevertheless, the power is high enough to demonstrate conclusively that methylacetylide radical has an electron affinity that is greater than 2.60 eV, i.e., $\text{EA}(\text{CH}_3\text{C}\equiv\text{C}) \geq 2.60$ eV.

We have also considered the degree of scrambling using $\text{CD}_3\text{C}\equiv\text{CH}$ as the ion precursor. Again, the mass resolution is similar to that in Figure 3. As before, we fix laser power and the value of V_{slit} . From 2.0 nA of the ion of m/z 41, we record an electron count rate of 160/s. From 1.6 nA of the ion of m/z 42, we see 23 counts/s. We conclude that the peak corresponding to m/z 41 is $\geq 85\%$ CD_2CCH^- and that corresponding to m/z 42 is $\geq 85\%$ $\text{CD}_3\text{C}\equiv\text{C}^-$. A summary of our ion separation and identification scheme may be seen in Table I.

The photodetachment spectra of the series of anions CH_2CCH^- , CH_2CCD^- , and CD_2CCH^- are presented in Figures 4–9. For all three ions, low-resolution spectra are shown over the entire (0.0–2.54 eV) electron-energy range in order to establish that there is only one electronic state of the propargyl radical accessed upon detachment. The high-resolution spectra are over a smaller energy range and show the spectral features more clearly. Figure 4 shows a low-resolution PES of CH_2CCH^- obtained by using $\text{CH}_3\text{C}\equiv\text{CH}/\text{O}_2$ as the ion source gas. Plotted is the total number of electrons counted vs. the center of mass (COM) kinetic energy of the detached electrons. Note that in the spectrum, kinetic energy increases to the right, with the highest possible value of electron COM kinetic energy equal to the laser energy (in this case 2.540 eV). It can be seen in Figure 4 that there is an apparent vibrational progression in the CH_2CCH^- spectrum. Figure 5, a high-resolution PES of the same ion, shows this vibrational progression more clearly. The details of this spectrum are quite complicated. Of the 12 normal modes of C_3H_3^- , any of the a' vibrations could be excited. We find clear evidence for only one active mode, however. Other vibrational modes and numerous rotations are excited as well but cannot be resolved or fit into a progression. The resolution of our spectrometer is roughly 200 cm^{-1} , and even the sharpest feature in Figure 5, peak D, is not simple. We notice that the first peaks in Figure 5 are quite broadened followed by a sharpening up at features D–F. We do not understand this. No features to the right of A are ever resolved, and the spectrum in this region varies markedly with our ion source conditions. The features in this spectrum are labeled A–M. The COM kinetic energies and splittings between these peaks are recorded in Table II.

Preliminary results from this data give a raw EA for CH_2CCH^- of $2.540 - 1.647$ eV, or 0.893 ± 0.019 eV, where it is conjectured

Table II. Peak Positions from CH_2CCH^- and CD_2CCH^- Photodetachment Spectra

peak	$\text{CH}_2\text{CCH}^- \rightarrow \text{CH}_2\text{CCH}$		$\text{CD}_2\text{CCH}^- \rightarrow \text{CD}_2\text{CCH}$	
	COM kinetic energy, eV	ΔE , cm^{-1}	COM kinetic energy, eV	ΔE , cm^{-1}
A	1.647 ± 0.019		1.633 ± 0.016	
B	1.578 ± 0.019	550 ± 220	1.567 ± 0.016	530 ± 180
C	1.521 ± 0.014	460 ± 190	1.506 ± 0.014	500 ± 180
D	1.454 ± 0.013	540 ± 150	1.441 ± 0.014	530 ± 160
E	1.395 ± 0.013	480 ± 150	1.379 ± 0.014	500 ± 160
F	1.327 ± 0.013	550 ± 150	1.320 ± 0.012	480 ± 140
G	1.264 ± 0.013	510 ± 150	1.256 ± 0.014	520 ± 140
H	1.196 ± 0.015	550 ± 160	1.188 ± 0.014	550 ± 160
I	1.139 ± 0.015	460 ± 170	1.126 ± 0.014	500 ± 160
J	1.072 ± 0.015	540 ± 170	1.067 ± 0.017	480 ± 180
K	1.013 ± 0.015	480 ± 170	1.000 ± 0.019	540 ± 200
L	0.941 ± 0.018	580 ± 190		
M	0.876 ± 0.021	530 ± 220		

that peak A corresponds to a transition from the ground vibrational state of the ion to the ground vibrational state of the neutral molecule. This conclusion implies the electrons detached with higher kinetic energy (i.e., to the right of peak A in Figure 5) are due to detachment from vibrationally or rotationally excited ions. In addition, because the splittings between peaks A–M are approximately constant, we assign these to a single vibrational progression in an as yet unidentified mode in the radical CH_2CCH . We have fit this set of features as an anharmonic potential. This function, $G(v) = \omega_e(v + 0.5) + \omega_e x_e(v + 0.5)^2$, gives an excellent fit to peaks A–K with $\omega_e = 510 \text{ cm}^{-1}$ and $\omega_e x_e = 0.6 \text{ cm}^{-1}$. Given the widths of the peaks in Figure 5 (see Table II), we see no reason not to treat this progression as arising from a simple harmonic oscillator. Using peaks A–K and assuming no anharmonicity, we find a vibrational splitting of 0.063 ± 0.001 eV (510 cm^{-1}). We have only used peaks A–K since peaks L and M are increasingly difficult to identify and because we will be comparing these results to those for CD_2CCH^- , for which only peaks A–K are clearly visible.

It should be pointed out that we have taken spectra for the ion of m/z 39 resulting from a $\text{CH}_2=\text{C}=\text{CH}_2/\text{O}_2$ mixture as well as from $\text{CH}_3\text{C}\equiv\text{CH}/\text{O}_2$. The PES of the m/z 39 ion from allene is identical with that from methylacetylene (Figure 5). This supplies additional evidence that the ion we are looking at is indeed CH_2CCH^- , since it is difficult to imagine producing $\text{CH}_3\text{C}\equiv\text{C}^-$ from allene.

Figures 6 and 7 show low- and high-resolution photodetachment spectra for the ion CD_2CCH^- generated from a $\text{CD}_3\text{C}\equiv\text{CH}/\text{O}_2$ mixture. Both spectra are remarkably similar to those from CH_2CCH^- . The high-resolution spectrum shows a comparable vibrational progression, with peaks labeled A–K. Their COM kinetic energies and splittings are also collected in Table II. The preliminary results from this spectrum give an EA for CD_2CCH^- of $2.540 - 1.633$ eV, or 0.907 ± 0.016 eV. In addition, the vibrational mode in CD_2CCH has a harmonic frequency of 0.063 ± 0.001 eV (510 cm^{-1}). It can be seen in Table II that all of the peaks in the CD_2CCH^- spectrum are lower in COM kinetic energy than the corresponding ones in the CH_2CCH^- spectrum. This shift probably results from changes in zero-point energies.

In Figures 8 and 9 are depicted low- and high-resolution PES of the ion CH_2CCD^- obtained from a mixture of $\text{CH}_3\text{C}\equiv\text{CD}$ and O_2 . It is immediately obvious that this spectrum is quite different from those of CH_2CCH^- and CD_2CCH^- . This will be very important in our discussion of the ion geometry. Although some hint of a vibrational structure can be seen in the high-resolution spectrum, we consider it not well-enough resolved to be analyzed. Therefore, only an approximate EA for CH_2CCD^- of $2.540 - 1.66$ eV, or 0.88 ± 0.15 eV, is assigned. The point used for this value is shown by the arrow in Figure 9.

Discussion

From the appearance of the vibrational structure of the photodetachment spectra of the series CH_2CCH^- , CH_2CCD^- , and

(21) B. K. Janousek, J. I. Brauman, and J. Simons, *J. Chem. Phys.*, **71**, 2057 (1979).

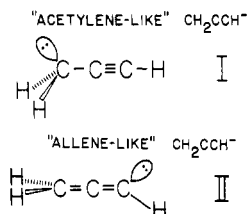


Figure 10. Proposed valence structures for the $C_3H_3^-$ ion. Ion I is the "acetylene-like" structure, while ion II is the "allene-like" structure.

CD_2CCH^- , we would like to consider the geometric structure of these anions. In order to proceed, the structure of the corresponding radical (CH_2CCH) must be established. In fact, since photoelectron spectroscopy only shows geometry differences, information about the structure of either the radical or the anion must be known before conclusions concerning the geometry of the other can be deduced. A brief discussion of the structure of the CH_2CCH radical follows.

The possible valence structures of CH_2CCH are $CH_2C\equiv CH$, an acetylene-like structure (presumably C_{2v} and planar), and $CH_2=C=CH$, an allene-like structure (of C_s symmetry and nonplanar). If the structure is indeed planar and acetylene-like, we would expect considerable resonance stabilization due to delocalization of the lone electron into the π system. Collin and Lossing²² prepared the C_3H_3 radical from Hg-photosensitized decomposition of allene ($Hg^* + CH_2=C=CH_2$) and allowed it to react with methyl radical (CH_3). The only product they detected was $CH_3CH_2C\equiv CH$. This is strong evidence that CH_2CCH has the structure $CH_2-C\equiv CH$, since the allene-like structure ($CH_2=C=CH$) would have been expected to yield primarily $CH_2=C=CHCH_3$. In addition, several authors have measured the "resonance energy" of the propargyl radical¹⁻³ as approximately 8.7–9.6 kcal/mol. This implies delocalization of the b_1 "p-like" electron of the CH_2 group into the π system and thus a nearly planar structure for the propargyl radical. Jacox and Milligan⁷ report a C–H stretching frequency for the C_3H_3 radical generated from allene of 3310 cm^{-1} . The only hydrocarbon C–H stretch normally found at these high frequencies are acetylenic hydrogens. For comparison,¹⁸ the C–H stretch in methylacetylene is 3334 cm^{-1} . This is another argument in favor of the acetylene-like structure for CH_2CCH . In addition, an ab initio molecular orbital calculation done by Bernardi et al.²³ has predicted a planar structure $CH_2C\equiv CH$ for the C_3H_3 radical. For the purposes of our discussion, then, we will assume that C_3H_3 has a planar, acetylene-like structure, i.e., the propargyl radical. The ground state of the propargyl radical is \tilde{X}^2B_1 .

In an analogous fashion, the CH_2CCH^- ion has two likely structures (see Figure 10). One is acetylene-like, $CH_2C\equiv CH$ (I), with C_1 having sp^3 hybridization and C_3 having sp hybridization. [For clarity of discussion, we will refer to the methylene carbon (CH_2) as C_1 and the methylene hydrogens as H_1 and H_2 . The middle carbon atom is called C_2 , while the terminal carbon is C_3 , and the hydrogen on it is H_3]. The other is allene-like, $CH_2=C=CH^-$ (II), with both C_1 and C_3 having sp^2 hybridization. Several theoretical treatments²⁴⁻²⁷ predict the allenic structure (II) to be the more stable. Hopkinson et al.²⁴ on the basis of a split-valence shell 4-31G basis set Hartree-Fock calculation, find structure I to be 9 kcal/mol higher in energy than the allenic structure (II). The acetylenic structure (I) did not show a minimum on the potential surface. Bushby et al.²⁵ have also used a self-consistent field (SCF) method and likewise concluded

structure II to be more stable. Constraining the CH_2 moiety to lie in the plane of the carbon skeleton, they²⁵ found H_3 to be out of the plane by 55° . Wilmhurst and Dykstra,²⁶ in a very careful study using SCF and correlated self-consistent electron pair (SCEP) methods, came to a similar conclusion, except that they allowed the CH_2-C-C angle to vary. They found the two hydrogens to vary from planarity by 3° , a $C_1-C_2-C_3$ angle of 176° , and a $C_2-C_3-H_3$ angle of 121° . Finally, an experimental ^{13}C NMR study²⁸ of $C_3H_3-Li^+$ in CCl_4 solution gave strong evidence that the carbanion in solution was allenic (II) and not propargyl (I).

Because of the large Franck-Condon envelope observed for each of our PES (Figure 5, 7, and 9), we conclude that there is a significant geometry change between the equilibrium structures of CH_2CCH^- and the propargyl radical. Both proposed structures for the anion $C_3H_3^-$, I and II, differ from that of propargyl C_3H_3 and therefore fit this criterion.

Should the propargyl anion possess a flat, C_{2v} structure like the neutral molecule, we would expect to find a structureless, vertical transition in the photodetachment spectrum. This is not observed (Figure 5). On the other hand if the ion I featured a pyramidal C (like that²⁹ of CH_3^-), it would differ from that of the propargyl radical primarily due to bending of the methylene hydrogens out-of-plane. If this is the case, we would predict that the vibrational structure observed in Figure 5 (for $C_3H_3^-$) is due to excitation in a CH_2 wag in the neutral molecule (just like CH_3^-). This mode might be expected to lie somewhere in the range of $500\text{--}1000\text{ cm}^{-1}$, by comparison to other CH_2 wags (e.g., CH_2 wag in allene¹⁸ is 841.8 cm^{-1}). The vibronic splittings we observe (510 cm^{-1}) seem possible for this mode. However, upon deuteration of the CH_2 moiety, we expect a significant shift in the frequency of this mode. Typically deuterium substitution causes an energy shift of about 25% for a bend. As an illustrative example¹⁸ of this, the b_{1u} CH_2 wag in $CH_2=CH_2$ has a frequency of 949 cm^{-1} , while the frequency of the b_{1u} CD_2 wag in $CD_2=CD_2$ is 720 cm^{-1} ; an energy difference of 24%. Inspection of the data from the PES of CD_2CCH^- extracted from $CD_3C\equiv CH$ (Table II and Figure 7) clearly shows no such isotope shift. Note that the vibrational spacings are virtually identical with those from $C_3H_3^-$. We conclude that the structure of the anion $C_3H_3^-$ is not similar to structure I.

The allenic structure (II) differs from that of the propargyl radical by an out-of-plane deformation of H_3 . If this is the case in the anion, we expect that the vibrational structure evident in Figure 5 is due to a $C_2-C_3-H_3$ out-of-plane bend in the final propargyl radical. Again, the vibrational frequency we have observed (510 cm^{-1}) is not unreasonable by comparison with other C–H bends (e.g., the $C\equiv C-H$ bend, ω_9 , reported¹⁸ in $CH_3C\equiv CH$ is 633 cm^{-1}). Upon deuteration of the C–H moiety in CH_2CCH^- , we expect an isotopic shift in the vibronic spacing exhibited in our PES of about 25%. [The vibrational frequency¹⁸ of the C–D bend (ω_9) in $CH_3C\equiv C-D$ is 498 cm^{-1} .] Inspection of the data obtained for CH_2CCD^- prepared from $CH_3C\equiv CD$ (see Figure 9) shows a large change from that for CH_2CCH^- (Figure 5). The frequency of the active vibrational mode has apparently decreased upon deuteration of the C–H moiety. We can no longer discern a vibrational progression even though our instrumental resolution is about 200 cm^{-1} . Another reasonable assignment for the 510-cm^{-1} mode is some sort of carbon skeletal motion. Because we have observed a significant shift in the photoelectron spectrum upon deuteration, we are able to exclude this type of motion as a possibility in assigning the active vibrational mode.

We conclude that the major change upon electron detachment from CH_2CCH^- is the excitation of a low-frequency C–H vibration involving H_3 . This is consistent with the evidence from matrix isolation spectroscopy⁷ of C_3H_3 . Two modes at 548 and 688 cm^{-1}

(22) J. Collin and F. P. Loosing, *Can. J. Chem.*, **35**, 778 (1959).

(23) F. Bernardi, C. M. Camaggi, and M. Tiecco, *J. Chem. Soc., Perkin Trans. 2*, 518 (1974).

(24) A. C. Hopkinson, M. H. Lien, K. Yates, P. G. Mezey, and I. G. Csizmadia, *J. Chem. Phys.*, **67**, 517 (1977).

(25) R. J. Bushby, A. S. Patterson, G. J. Ferber, A. J. Duke, and G. H. Whitman, *J. Chem. Soc., Perkin Trans. 2*, 807 (1978).

(26) J. K. Wilmhurst and C. E. Dykstra, *J. Am. Chem. Soc.*, **102**, 4668 (1980).

(27) W. Grundler, *Tetrahedron*, **26**, 2291 (1970).

(28) J. P. C. M. van Dongen, H. W. D. van Dijkman, and M. J. A. de Bie, *Recl. Trav. Chim. Pays-Bas*, **93**, 29 (1974).

(29) G. B. Ellison, P. C. Engelking, and W. C. Lineberger, *J. Am. Chem. Soc.*, **100**, 2526 (1978).

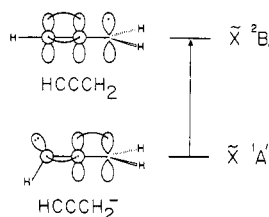


Figure 11. Qualitative picture of the \hat{X}^1A' ($\text{CH}_2=\text{C}=\text{CH}^-$) \rightarrow \hat{X}^2B_1 ($\text{CH}_2\text{C}\equiv\text{CH}$) transition using generalized valence bond (GVB) ideas (see ref 30 and 31).

were considered as C-H deformations in the propargyl radical. These arguments favor an allenic structure (II) for the CH_2CCH^- ion. The ground state of this ion is \hat{X}^1A' . Upon detachment, the system makes a transition from the bent \hat{X}^1A' state of $\text{CH}_2=\text{C}=\text{CH}^-$ to the flat \hat{X}^2B_1 state of the propargyl radical, $\text{CH}_2-\text{C}\equiv\text{CH}$. Figure 11 depicts this process with diagrams based on generalized valence bond (GVB) ideas^{30,31} for C_3H_3^- and C_3H_3 .

We now turn to some of the thermodynamic information derivable from the photoelectron spectra. First consider the raw electron affinities. For both $\text{CH}_2=\text{C}=\text{CH}^-$ and $\text{CD}_2=\text{C}=\text{CH}^-$ (Figure 5 and 7), we have assigned the peaks labeled A as the origin, i.e., as corresponding to $\text{C}_3\text{H}_3^- \hat{X}^1A' (v''=0) \rightarrow \text{C}_3\text{H}_3 \hat{X}^2B_1 (v'=0)$. Peaks in the progression (B, C, ...) then correspond to overtones in v' ($v'=1, 2, \dots$). From Figure 5 for $\text{CH}_2=\text{C}=\text{CH}^-$ (allenyl anion), it is seen that peak A is the first clearly distinguishable feature in the spectrum. Because no break in the vibrational spacing is seen, it is reasonable to conjecture that peaks A-M all result from an excitation of a single mode. The detached electrons detected to the high-electron-energy side of feature A (Figures 5 and 7) are then assignable as unresolved transitions originating from vibrationally excited ions ("hot bands"). Thus they are from some vibrational mode(s) in the negative ion with $v'' \neq 0$. Our ion source has been characterized¹⁶ by a vibrational temperature of roughly 450 K. It is quite likely that a number of low-frequency modes in C_3H_3^- are populated. Detachment from a distribution of rotationally and vibrationally excited ions would lead to a set of convoluted features to the high-energy side of the origin, peak A. We should stress that we cannot absolutely identify the origin peak, but given that there is a long harmonic vibrational progression (A-M) and no anomalous break in the shape of the Franck-Condon envelope, peak A is the most reasonable origin. As will be seen below, the $\Delta H^\circ_{\text{acid}}(\text{H}-\text{CH}_2\text{C}\equiv\text{CH})$ derived by using the EA from peak A corresponds well with all other thermodynamic data for $\text{CH}_3\text{C}\equiv\text{CH}$.

Our assignment of the peak labeled A as the origin in the spectrum for $\text{CD}_2=\text{C}=\text{CH}^- \hat{X}^1A' \rightarrow \text{CD}_2\text{C}\equiv\text{CH} \hat{X}^2B_1$ (Figure 7) is not as obvious as it was in the spectrum in Figure 5 for $\text{CH}_2=\text{C}=\text{CH}^-$. We have recorded this photoelectron spectrum several times, and peak A is always present. What may appear to be an additional peak to the right of peak A is not observed consistently. Therefore we assign all the electron detachment to the high side of peak A in Figure 7 as hot bands. An additional argument to support this conclusion is that the difference in EA between CH_2CCH to CD_2CCH should only result from differences in the zero-point energies (roughly 10–20 meV). Choosing peak A as the origin in Figure 7 results in a small (0.014 eV) difference in EA for the two radicals.

The peak for $\text{CH}_2=\text{C}=\text{CD}^- \hat{X}^1A' (v''=0) \rightarrow \text{CH}_2\text{C}\equiv\text{CD} \hat{X}^2B_1 (v'=0)$ cannot be picked out at all (Figure 9). Consequently we report an origin of 1.66 ± 0.15 eV, with rather wide error bars. The origin is depicted by the arrow in Figure 9.

Now, we will discuss the corrections to the raw electron affinities derived from our data. It has already been mentioned that the peaks seen in the spectra are certainly wider than our instrumental

Table III. Final Experimental Values

species	EA, eV	$\text{C}\equiv\text{C}-\text{H}$ bending frequency, cm^{-1}
$\text{CH}_2-\text{C}\equiv\text{CH}$	0.893 ± 0.025	510
$\text{CD}_2-\text{C}\equiv\text{CH}$	0.907 ± 0.023	510
$\text{CH}_2-\text{C}\equiv\text{CD}$	0.88 ± 0.15	

fwhm (0.020–0.025 eV). The peak width may be attributed to the presence of many unresolved rotational bands, possible spin-orbit multiplicities, and sequence hot bands. The EA of a molecule is, by definition, the energy difference between the lowest rovibronic level of the lowest spin-orbit component of the ion and the corresponding state of the neutral molecule. For asymmetric tops such as the propargyl radical and the allenic ion, little is known of the rotational constants or vibrational frequencies. As a result we can only estimate most of these corrections and the corresponding errors. The contribution to our final error bars from each of these factors is as follows: rotational correction ± 0.005 eV, vibrational sequence band correction ± 0.015 , and spin-orbit correction ± 0.001 eV. The couplings of spin to other angular momenta are considered to be negligible. Table III collects the final values for the electron affinities and vibrational frequencies for C_3H_3 and its deuterated isomers.

The enthalpy for the process $\text{HA} \rightarrow \text{A}^- + \text{H}^+$ is defined as the gas-phase acidity ($\Delta H^\circ_{\text{acid}}$). From this definition, the thermodynamic cycle

$$\Delta H^\circ_{\text{acid}}(\text{HA}) = \text{IP}(\text{H}) + \Delta H^\circ(\text{HA}) - \text{EA}(\text{A}) \quad (2)$$

can be derived, where the ionization potential of hydrogen³² is known to be 313.6 kcal/mol. If either ΔH° , the A-H bond strength, or $\Delta H^\circ_{\text{acid}}$ is known, the other may be derived if $\text{EA}(\text{A})$ is available.

The heat of formation of the propargyl radical has been studied extensively; in a shock tube study,¹ by very low-pressure pyrolysis (VLPP),^{2,3} and by appearance potential-kinetic energy analysis upon electron impact.⁴ King^{2,3} summarized this to arrive at $\Delta H^\circ_{f,298}(\text{propargyl}) = 81.5 \pm 1.0$ kcal/mol. Because³³ the $\Delta H^\circ_{f,298}(\text{CH}_2=\text{C}=\text{CH}_2)$ is 45.92 kcal/mol and $\Delta H^\circ_{f,298}(\text{CH}_3\text{C}\equiv\text{CH})$ is 44.32 kcal/mol, the heats of formation of $\text{CH}_2\text{C}\equiv\text{CH}$ and H have been used to calculate bond-dissociation energies for $\text{CH}_2=\text{C}=\text{CH}_2$ and $\text{CH}_3\text{C}\equiv\text{CH}$. These are $\Delta H^\circ(\text{H}-\text{CHCCH}_2) = 87.7 \pm 1.0$ kcal/mol and $\Delta H^\circ(\text{H}-\text{CH}_2\text{CCH}) = 89.3 \pm 1.0$ kcal/mol. The ion heat of formation is obtained³⁴ from the EA as follows:

$$\Delta H^\circ_{f,298}(\text{CH}_2\text{C}\equiv\text{CH}) - \Delta H^\circ_{f,298}(\text{CH}_2=\text{C}=\text{CH}^-) = \text{EA}(\text{CH}_2\text{C}\equiv\text{CH}) + \frac{1}{2}RT \quad (3)$$

In (3) $\frac{1}{2}RT$ is the heat capacity of the electron, 1.481 kcal/mol. Then it follows from our $\text{EA}(\text{CH}_2\text{C}\equiv\text{CH})$ of 0.893 ± 0.025 eV that the heat of formation of the allenic ion, $\Delta H^\circ_{f,298}(\text{CH}_2=\text{C}=\text{CH}^-)$, is 59.4 ± 1.2 kcal/mol.

Using these results and our values for the electron affinities, one calculates a gas-phase acidity of allene $\Delta H^\circ_{\text{acid}}(\text{H}-\text{CH}=\text{C}=\text{CH}_2) = 380.7 \pm 1.2$ kcal/mol, and that of methylacetylene $\Delta H^\circ_{\text{acid}}(\text{H}-\text{CH}_2\text{C}\equiv\text{CH}) = 382.3 \pm 1.2$ kcal/mol. As was pointed out earlier, Bartmess et al.⁸ have measured $\Delta H^\circ_{\text{acid}}(\text{CH}_3\text{C}\equiv\text{C}-\text{H}) = 379.6 \pm 2$ kcal/mol. It has been estimated¹⁰ that $\Delta H^\circ_{\text{acid}}(\text{H}-\text{CH}_2\text{C}\equiv\text{CH})$ is greater than $\Delta H^\circ_{\text{acid}}(\text{H}-\text{C}\equiv\text{CCH}_3)$ by roughly 3 kcal/mol. As mentioned earlier, $\text{CH}_3\text{C}\equiv\text{C}^-$ does not detach with 2.707-eV photons. Because it is difficult for us to detect electrons with energies less than 0.1 eV, we can say that $\text{EA}(\text{CH}_3\text{C}\equiv\text{C}) > 2.60$ eV. Using this fact and $\Delta H^\circ_{\text{acid}}$ of 379 kcal/mol in (2), we find $\Delta H^\circ(\text{H}-\text{C}\equiv\text{CCH}_3) > 125$ kcal/mol.

(32) D. R. Stull and H. Prophet, "JANAF Thermochemical Tables", 2nd ed., National Bureau of Standards, Washington, DC 1971.

(33) H. M. Rosenstock, K. Draxl, B. W. Steiner, and J. T. Herron, *J. Phys. Chem. Ref. Data, Suppl.*, 6 (1977).

(34) S. G. Lias, in "Kinetics of Ion-Molecule Reactions", P. Ausloos, Ed., Plenum Publishing, New York, 1979, pp 223–254.

(30) W. A. Goddard, III, T. H. Dunning, Jr., W. J. Hunt, and P. J. Hay, *Acc. Chem. Res.*, 6, 368 (1973).

(31) W. A. Goddard, III, and L. B. Hading, *Ann. Rev. Phys. Chem.*, 29, 363 (1978).

Conclusion

A number of results can be summarized here. By employing deuterated ion precursors we are able to prepare selectively CH_2CCH^- or CH_3CC^- . An ion beam of the former is photodetached by 488-nm laser light, while a beam of the latter species is not. Examination of the photoelectron spectra of CH_2CCH^- , CD_2CCH^- , and CH_2CCD^- allows us to deduce the structures of the ions. On the basis of present evidence for the structure of the propargyl radical, $\text{CH}_2\text{C}\equiv\text{CH}$, and isotope effects observed in our spectra, we conclude that the detaching species is $\text{CH}_2=\text{C}=\text{CH}^-$ and not $^-\text{CH}_2\text{C}\equiv\text{CH}$. The vibration excited in the resulting $\text{CH}_2\text{C}\equiv\text{CH}$ resulting from detachment is a harmonic mode (510 cm^{-1}) and is most likely the $\text{C}\equiv\text{C}-\text{H}$ out-of-plane deformation. The electron affinities of several isotopically substituted propargyl radicals are collected together in Table III. Gas-phase acidities of $\text{CH}_2=\text{C}=\text{CH}_2$ and $\text{CH}_3\text{C}\equiv\text{CH}$ are computed. We are unable to detach $\text{CH}_3\text{C}\equiv\text{C}^-$ and conclude that $\text{EA}(\text{CH}_3\text{C}\equiv\text{C}^-) > 2.60\text{ eV}$. On the basis of this and a conjecture

for the $\Delta H^\circ_{\text{acid}}(\text{H}-\text{CCCH}_3)$, we conclude that $\Delta H^\circ(\text{H}-\text{CCCH}_3) > 125\text{ kcal/mol}$.

Acknowledgment. We thank H. Benton Ellis, Jr., for his assistance and constant advice in operating the photoelectron spectrometer. Suzanne Paulson and Prof. Gary A. Molander assisted us in the synthesis and purification of methylacetylene- d_1 . We would like to acknowledge Prof. John Bartmess for a helpful discussion of the gas-phase acidity of methylacetylene. Financial support for this work was provided by the Research Corp., the donors of the Petroleum Research Foundation, administered by the American Chemical Society, and the United States Department of Energy (Contract DE-AC02-80ER10722). G.B.E. thanks the Alfred P. Sloan Foundation for a Fellowship.

Registry No. $\text{CH}_2=\text{C}=\text{CH}^-$, 64066-06-4; $\text{CD}_2=\text{C}=\text{CH}^-$, 85048-63-1; $\text{CH}_2=\text{C}=\text{CD}^-$, 85048-64-2; $\text{HC}\equiv\text{CCH}_2^-$, 2932-78-7; $\text{HC}\equiv\text{CCD}_2^-$, 15650-79-0; $\text{DC}\equiv\text{CCH}_2^-$, 85048-65-3; CH_3CCH , 74-99-7; $\text{CH}_2=\text{C}=\text{CH}_2$, 463-49-0; $\text{CH}_3\text{C}\equiv\text{C}^-$, 7299-37-8; $\text{CD}_3\text{C}\equiv\text{CH}$, 13025-73-5; $\text{CH}_3\text{C}\equiv\text{C}^-$, 36147-87-2.

Dynamic and Structural Properties of Polymerized Phosphatidylcholine Vesicle Membranes

Akihiro Kusumi,^{1a} Maninder Singh,^{1b} David A. Tirrell,^{1c} Gunther Oehme,^{1b} Alok Singh,^{1b} N. K. P. Samuel,^{1b} James S. Hyde,^{1a} and Steven L. Regen*^{1b}

Contribution from the Department of Chemistry, Marquette University, Milwaukee, Wisconsin 53233, the National Biomedical ESR Center, Department of Radiology, Medical College of Wisconsin, Milwaukee, Wisconsin 53226, and the Department of Chemistry, Carnegie-Mellon University, Pittsburgh, Pennsylvania 15213. Received September 7, 1982

Abstract: The phase transition, fluidity, and polarity properties of polymerized and nonpolymerized vesicle membranes derived from 1-palmitoyl-2-[12-(methacryloyloxy)dodecanoyl]-L- α -phosphatidylcholine (**1**), bis[12-(methacryloyloxy)dodecanoyl]-L- α -phosphatidylcholine (**2**), and 1,2-dipalmitoyl[N-2-(methacryloyloxy)ethyl]-DL- α -phosphatidylcholine (**3**) have been examined by means of differential scanning calorimetry and by the spin-labeling technique. Above 5°C aqueous multilamellar dispersions of **1**, **2**, and **3** show a broad-phase transition, no phase change, and a sharp transition, respectively. Polymerization of the methacrylate group causes a decrease in membrane fluidity in each case and an increase in the temperature of the gross phase change for **1** and **3**. Membrane fluidity in copolymerized vesicles of **1** and **2** decreases linearly with the mole fraction of **2** used. The polarity gradient in membranes of **3** is small; polarity gradients in membranes of **1** and **2** are large. Polymerization has no noticeable effect on these gradients. Fluidity gradients are also present in membranes of **1**, **2**, and **3** above 20°C . Polymerization alters the fluidity gradients in a manner which is comparable to lowering the temperature; it also reduces the ability of each membrane to bind [^{15}N]perdeuteriotemponone. These results are compared directly with the dynamic and structural properties found in conventional liposomes derived from dipalmitoylphosphatidylcholine and egg yolk phosphatidylcholine.

Polymerized forms of lipid bilayer vesicles have recently been described by several laboratories.²⁻⁹ Because of their enhanced stability, this unique class of polymers offers an attractive alternative to conventional liposomes as models for biological membranes, devices for solar energy conversion, and carriers of drugs.¹⁰⁻¹⁸ While considerable interest has centered around their synthetic design, polymerization behavior, gross morphology, entrapment efficiency, permeability, and stability, relatively little attention has focused on the dynamic and structural features of the membrane network.

In this paper we report the results of a spin-labeling study and a differential scanning calorimetry (DSC) analysis aimed at characterizing the phase transition, fluidity, and polarity properties of polymerized and nonpolymerized vesicle membranes derived from 1-palmitoyl-2-[12-(methacryloyloxy)dodecanoyl]-L- α -phosphatidylcholine (**1**), bis[12-(methacryloyloxy)dodecanoyl]-

L- α -phosphatidylcholine (**2**), and 1,2-dipalmitoyl[N-2-(methacryloyloxy)ethyl]-DL- α -phosphatidylcholine (**3**). Our reasons

(1) (a) National Biomedical ESR Center. (b) Marquette University. (c) Carnegie-Mellon University.

(2) Regen, S. L.; Czech, B.; Singh, A. *J. Am. Chem. Soc.* **1980**, *102*, 6638. Regen, S. L.; Singh, A.; Oehme, G.; Singh, M. *Biochem. Biophys. Res. Commun.* **1981**, *101*, 131. Regen, S. L.; Singh, A.; Oehme, G.; Singh, M. *J. Am. Chem. Soc.* **1982**, *104*, 791.

(3) Hub, H. H.; Hupfer, B.; Koch, H.; Ringsdorf, H. *Angew. Chem., Int. Ed. Engl.* **1980**, *19*, 938.

(4) Akimoto, A.; Dorn, K.; Gross, L.; Ringsdorf, H.; Schupp, H. *Angew. Chem., Int. Ed. Engl.* **1981**, *20*, 90.

(5) Johnston, D. S.; Sanghera, S.; Pons, M.; Chapman, D. *Biochim. Biophys. Acta* **1980**, *602*, 57.

(6) Lopez, E.; O'Brien, D. F.; Whitesides, T. H. *J. Am. Chem. Soc.* **1982**, *104*, 305. O'Brien, D. F.; Whitesides, T. H.; Klingbiel, R. T. *J. Polym. Sci., Polym. Lett. Ed.* **1981**, *19*, 94.

(7) Gros, L.; Ringsdorf, H.; Schupp, H. *Angew. Chem., Int. Ed. Engl.* **1981**, *20*, 305. Folda, T.; Gros, L.; Ringsdorf, M. *Makromol. Chem. Rapid Commun.* **1982**, *3*, 167.

* Alfred P. Sloan Fellow, 1982-1984.